Supporting Information

Anomalous Wavelength Scaling of Tightly-Coupled Terahertz Metasurfaces

Ji-Hun Kang[1†], Seo-Joo Lee[2], Bong Joo Kang[3], Won Tae Kim[3], Fabian Rotermund[3], and Q-Han Park[2*]

[1] Department of Physics, University of California at Berkeley, Berkeley, CA 94720, United States

[2] Department of Physics, Korea University, Seoul 02841, Republic of Korea

[3] Department of Physics, Korea Advanced Institute of Science and Technology, Daejeon 34141, Republic of Korea

[*] Corresponding author: qpark@korea.ac.kr

[†] Present address: Department of Physics and Astronomy, Seoul National University, Seoul 08826, Republic of Korea

1. Analytic theory on the transmission and reflection coefficients of the metasurface

Consider an *x*-polarized light incident normally onto the metasurface, as shown in Fig. 1 in the main text, and also in Fig. S1. We assume that the metasurface is made of perfectly electric conductor (PEC). For region I (incident region) and III (transmitted region), the Bloch's theorem allows us to expand the diffracted electromagnetic (EM) waves in a quantized form as,

$$\begin{aligned}\vec{H}_I &= \sqrt{\frac{\varepsilon_0}{\mu_0}}\sum_{m,n=-\infty}^{\infty}\left[\hat{y}\delta_{m0}\delta_{n0}e^{ik_0(z+h/2)}+\vec{R}_{mn}e^{-i\chi_{mn}(z+h/2)}\right]e^{i\phi_{mn}} \\ \vec{H}_{III} &= \sqrt{\frac{\varepsilon_0}{\mu_0}}\sum_{m,n=-\infty}^{\infty}\left[\vec{T}_{mn}e^{i\chi_{mn}(z-h/2)}\right]e^{i\phi_{mn}},\end{aligned} \tag{1.1}$$

where $\phi_{mn}\equiv\alpha_m\left(x-a/2\right)+\beta_n\left(y-b/2\right)$ and $k_0\equiv 2\pi/\lambda$. $\alpha_m\equiv 2\pi m/d_x$, $\beta\equiv 2\pi n/d_y$, and $\chi_{mn}\equiv\sqrt{k_0^2-\alpha_m^2-\beta_n^2}$ are momenta of diffracted waves in *x*, *y*, and *z* directions, respectively. Since we are considering that both *b* and $g_{x,y}$ are in sub-wavelength, we approximate EM waves in two light channels in the metasurface, denoted by $c^{(1)}$ and $c^{(2)}$ in Fig. S1, by using single-mode expansion. Note that higher-order waveguide modes decay rapidly in the metasurface, so that their contribution to the electromagnetic wave configuration in the metasurface becomes smaller with narrower *b* and $g_{x,y}$. Then, the field distribution in channel $c^{(1)}$ can be given by [1]

$$\begin{aligned}E_{xII}^{(1)} &= \sin\left(\frac{\pi y}{b}\right)\left(A_1e^{ik_1z}+B_1e^{-ik_1z}\right),\quad E_{yII}^{(1)}=0,\quad E_{zII}^{(1)}=0,\quad H_{xII}^{(1)}=0 \\ H_{yII}^{(1)} &= \frac{1}{k_0}\sqrt{\frac{\varepsilon_0}{\mu_0}}k_1\sin\left(\frac{\pi y}{b}\right)\left[A_1e^{ik_1z}-B_1e^{-ik_1z}\right], \\ H_{zII}^{(1)} &= \frac{i}{k_0}\sqrt{\frac{\varepsilon_0}{\mu_0}}\frac{\pi}{b}\cos\left(\frac{\pi y}{b}\right)\left[A_1e^{ik_1z}+B_1e^{-ik_1z}\right],\quad k_1\equiv\sqrt{k_0^2-\left(\frac{\pi}{b}\right)^2}\end{aligned} \tag{1.2}$$

and for channel $c^{(2)}$, it can be written as

$$
\begin{aligned}
&E_{xII}^{(2)} = A_2 e^{ik_0 z} + B_2 e^{-ik_0 z}, \quad E_{yII}^{(2)} = 0, \quad E_{zII}^{(2)} = 0, \\
&H_{xII}^{(2)} = 0, \quad H_{yII}^{(2)} = \sqrt{\frac{\varepsilon_0}{\mu_0}} \left[A_2 e^{ik_0 z} - B_2 e^{-ik_0 z} \right], \; H_{zII}^{(2)} = 0.
\end{aligned} \tag{1.3}
$$

Here, $A_{1,2}$ and $B_{1,2}$ are amplitudes of internal waveguide modes in two channels. Now, we can readily apply the boundary conditions. Continuity of E_x field at z=-h/2 gives

$$
\begin{aligned}
&-\frac{1}{k_0} \sum_{mn} \left(\beta_n R_{z,mn} - k_0 \delta_{m0} \delta_{n0} + \chi_{mn} R_{y,mn} \right) e^{i\phi_{mn}} \\
&= \sin\left(\frac{\pi y}{b} \right) \left[A_1 e^{-ik_1 h/2} + B_1 e^{ik_1 h/2} \right], \; \left(\text{on } c^{(1)} \right) \\
&= A_2 e^{-ik_0 h/2} + B_2 e^{ik_0 h/2}, \; \left(\text{on } c^{(2)} \right) \\
&= 0 \quad (\text{otherwise}),
\end{aligned} \tag{1.4}
$$

and at z=h/2, we have

$$
\begin{aligned}
&-\frac{1}{k_0} \sum_{mn} \left(\beta_n T_{z,mn} - \chi_{mn} T_{y,mn} \right) e^{i\phi_{mn}} \\
&= \sin\left(\frac{\pi y}{b} \right) \left[A_1 e^{ik_1 h/2} + B_1 e^{-ik_1 h/2} \right], \; \left(\text{on } c^{(1)} \right) \\
&= A_2 e^{ik_0 h/2} + B_2 e^{-ik_0 h/2}, \; \left(\text{on } c^{(2)} \right) \\
&= 0 \quad (\text{otherwise}).
\end{aligned} \tag{1.5}
$$

Also, continuity of E_y field at z=±h/2 yields

$$
\sum_{mn} \left(\chi_{mn} R_{x,mn} + \alpha_m R_{z,mn} \right) e^{i\phi_{mn}} = 0, \quad \sum_{mn} \left(\chi_{mn} T_{x,mn} - \alpha_m T_{z,mn} \right) e^{i\phi_{mn}} = 0. \tag{1.6}
$$

On the other hand, divergence-less of magnetic field gives

$$
\alpha_m R_{x,mn} + \beta_n R_{y,mn} - \chi_{mn} R_{z,mn} = 0, \quad \alpha_m T_{x,mn} + \beta_n T_{y,mn} + \chi_{mn} T_{z,mn} = 0. \tag{1.7}
$$

By combining Eq. (1.6) and (1.7), we can reduce R_{mn} and T_{mn} as the following:

$$
\begin{aligned}
R_{x,mn} &= -\frac{\alpha_m \beta_n}{\alpha_m^2 + \chi_{mn}^2} R_{y,mn}, \quad R_{z,mn} = \frac{\beta_n \chi_{mn}}{\alpha_m^2 + \chi_{mn}^2} R_{y,mn}, \\
T_{x,mn} &= -\frac{\alpha_m \beta_n}{\alpha_m^2 + \chi_{mn}^2} T_{y,mn}, \quad T_{z,mn} = -\frac{\beta_n \chi_{mn}}{\alpha_m^2 + \chi_{mn}^2} T_{y,mn}.
\end{aligned} \tag{1.8}
$$

Then, the first terms of Eq. (1.4) and (1.5) become

$$
\begin{aligned}
-\frac{1}{k_0} \sum_{mn} \left(\beta_n R_{z,mn} - k_0 \delta_{m0} \delta_{n0} + \chi_{mn} R_{y,mn} \right) e^{i\phi_{mn}} &= -\sum_{mn} \left(\frac{k_0 \chi_{mn}}{\alpha_m^2 + \chi_{mn}^2} R_{y,mn} e^{i\phi_{mn}} \right) + 1 \\
-\frac{1}{k_0} \sum_{mn} \left(\beta_n T_{z,mn} - \chi_{mn} T_{y,mn} \right) e^{i\phi_{mn}} &= \sum_{mn} \frac{k_0 \chi_{mn}}{\alpha_m^2 + \chi_{mn}^2} T_{y,mn} e^{i\phi_{mn}}.
\end{aligned} \tag{1.9}
$$

After inverse Fourier transform of Eq. (1.4) and (1.5), incorporated with (1.9), we can write *y*-component of R_{mn} and T_{mn} in terms of coefficients $A_{1,2}$ and $B_{1,2}$:

$$
\begin{aligned}
\frac{k_0 \chi_{mn}}{\alpha_m^2 + \chi_{mn}^2} R_{y,mn} - \delta_{m0} \delta_{n0} &= -Q_{mn} \left[A_1 e^{-ik_1 h/2} + B_1 e^{ik_1 h/2} \right] - \bar{Q}_{mn} \left[A_2 e^{-ik_0 h/2} + B_2 e^{ik_0 h/2} \right], \\
\frac{k_0 \chi_{mn}}{\alpha_m^2 + \chi_{mn}^2} T_{y,mn} &= Q_{mn} \left[A_1 e^{ik_1 h/2} + B_1 e^{-ik_1 h/2} \right] + \bar{Q}_{mn} \left[A_2 e^{ik_0 h/2} + B_2 e^{-ik_0 h/2} \right].
\end{aligned} \tag{1.10}
$$

Here, Q_{mn} and $\bar{Q}_{mn}$, the vector-dependencies between external diffracted waves and internal waveguide modes in two channels, are given by

$$
Q_{mn} \equiv \frac{1}{d_x d_y} \int_0^a dx \int_0^b dy \sin\left(\frac{\pi y}{b} \right) e^{-i\phi_{mn}}, \qquad \bar{Q}_{mn} \equiv \frac{1}{d_x d_y} \int_{a+w}^{a+w+g_x} dx \int_0^{d_y} dy e^{-i\phi_{mn}}. \tag{1.11}
$$

Equation (1.10) gives the relationship between the diffracted waves and waveguide modes in the metasurface. Specifically, with the fact that $Q_{00} = 2ab / d_x d_y \pi$ and $\bar{Q}_{00} = g_x / d_x$, we can obtain the zero-th order transmittance and reflectance that are given in Eq. (2) of the main text,

$$T_{y,00} = \frac{2ab}{d_x d_y \pi}\left[A_1 e^{ik_1 h/2} + B_1 e^{-ik_1 h/2} \right] + \frac{g_x}{d_x}\left[A_2 e^{ik_0 h/2} + B_2 e^{-ik_0 h/2} \right],$$
$$R_{y,00} = 1 - \frac{2ab}{d_x d_y \pi}\left[A_1 e^{-ik_1 h/2} + B_1 e^{ik_1 h/2} \right] - \frac{g_x}{d_x}\left[A_2 e^{-ik_0 h/2} + B_2 e^{ik_0 h/2} \right]. \quad (1.12)$$

In order to fix undetermined coefficients $A_{1,2}$ and $B_{1,2}$, we can go over the same procedure by using the continuity of tangential magnetic fields at two interfaces. Continuity of H_y field at z=-h/2 gives

$$\begin{aligned} &\sum_{mn}\left[\delta_{m0}\delta_{n0} + R_{y,mn} \right] e^{i\phi_{mn}} \\ &= \frac{k_1}{k_0}\sin\left(\frac{\pi y}{b}\right)\left[A_1 e^{-ik_1 h/2} - B_1 e^{ik_1 h/2} \right] \quad \left(\text{on } c^{(1)}\right), \\ &= A_2 e^{-ik_0 h/2} - B_2 e^{ik_0 h/2} \quad \left(\text{on } c^{(2)}\right). \end{aligned} \quad (1.13)$$

Also, from the continuity at z=h/2, we have

$$\begin{aligned} &\sum_{mn} T_{y,mn} e^{i\phi_{mn}} \\ &= \frac{k_1}{k_0}\sin\left(\frac{\pi y}{b}\right)\left[A_1 e^{ik_1 h/2} - B_1 e^{-ik_1 h/2} \right] \quad \left(\text{on } c^{(1)}\right), \\ &= A_2 e^{ik_0 h/2} - B_2 e^{-ik_0 h/2} \quad \left(\text{on } c^{(2)}\right). \end{aligned} \quad (1.14)$$

Previously, we have used the Fourier transform that is identical to the projection onto the plane-wave basis. This was possible because the electric field in the metasurface is defined everywhere including inside the metal, whereas the magnetic field is defined only in two light channels. Therefore, for the magnetic field, instead of Fourier transform, we make use of projection of the plane-wave onto waveguide modes [1, 2]. From Eq. (1.13), projections onto the modes in $c^{(1)}$ and $c^{(2)}$ respectively give

$$\sum_{mn}\left[\delta_{m0}\delta_{n0}+R_{y,mn}\right]P_{mn}=\frac{k_1}{k_0}\left[A_1e^{-ik_1h/2}-B_1e^{ik_1h/2}\right],$$
$$\sum_{mn}\left[\delta_{m0}\delta_{n0}+R_{y,mn}\right]\bar{P}_{mn}=\left[A_2e^{-ik_0h/2}-B_2e^{ik_0h/2}\right], \tag{1.15}$$

and from Eq. (1.14), we have

$$\sum_{mn}T_{y,mn}P_{mn}=\frac{k_1}{k_0}\left[A_1e^{ik_1h/2}-B_1e^{-ik_1h/2}\right],$$
$$\sum_{mn}T_{y,mn}\bar{P}_{mn}=\left[A_2e^{ik_0h/2}-B_2e^{-ik_0h/2}\right]. \tag{1.16}$$

Here, two vector-dependencies P_{mn} and $\bar{P}_{mn}$ are defined by

$$P_{mn}\equiv\frac{2}{ab}\int_0^a dx\int_0^b dy\sin\left(\frac{\pi y}{b}\right)e^{i\phi_{mn}}=\frac{2d_xd_y}{ab}Q_{mn},$$
$$\bar{P}_{mn}\equiv\frac{1}{g_xd_y}\int_{a+\mathrm{w}}^{a+\mathrm{w}+g_x}dx\int_0^{d_y}dye^{i\phi_{mn}}=\frac{d_x}{g_x}\bar{Q}_{mn}. \tag{1.17}$$

Combining Eq. (1.12), (1.15), and (1.16), we can obtain a coupled equation for coefficients $A_{1,2}$ and $B_{1,2}$:

$$A_1e^{-ik_1h/2}\left(W+\frac{k_1}{k_0}\right)+B_1e^{ik_1h/2}\left(W-\frac{k_1}{k_0}\right)+A_2e^{-ik_0h/2}\bar{W}+B_2e^{ik_0h/2}\bar{W}=\frac{8}{\pi},$$
$$A_1e^{ik_1h/2}\left(W-\frac{k_1}{k_0}\right)+B_1e^{-ik_1h/2}\left(W+\frac{k_1}{k_0}\right)+A_2e^{ik_0h/2}\bar{W}+B_2e^{-ik_0h/2}\bar{W}=0,$$
$$A_1e^{-ik_1h/2}\bar{V}+B_1e^{ik_1h/2}\bar{V}+A_2e^{-ik_0h/2}\left(V+1\right)+B_2e^{ik_0h/2}\left(V-1\right)=2,$$
$$A_1e^{ik_1h/2}\bar{V}+B_1e^{-ik_1h/2}\bar{V}+A_2e^{ik_0h/2}\left(V-1\right)+B_2e^{-ik_0h/2}\left(V+1\right)=0. \tag{1.18}$$

Four coupling factors are given by

$$W \equiv \sum_{m,n=-\infty}^{\infty} \frac{\alpha_m^2 + \chi_{mn}^2}{k_0 \chi_{mn}} Q_{mn} P_{mn} \approx \frac{8ab}{\pi^2 d_x d_y} + i \frac{4ad_y^2}{k_0 \pi b^3 d_x}, \quad V \equiv \sum_{m,n=-\infty}^{\infty} \frac{\alpha_m^2 + \chi_{mn}^2}{k_0 \chi_{mn}} Q_{mn} P_{mn} \approx g_x \left(\frac{1}{d_x} + i \frac{k_0}{\pi} \Omega \right),$$

$$\overline{V} \equiv \sum_{m,n=-\infty}^{\infty} \frac{\alpha_m^2 + \chi_{mn}^2}{k_0 \chi_{mn}} Q_{mn} \overline{P}_{mn} \approx \frac{2ab}{\pi d_x d_y} - i g_x \frac{2k_0 b}{\pi^2 d_y} \overline{\Omega}, \quad \overline{W} \equiv \sum_{m,n=-\infty}^{\infty} \frac{\alpha_m^2 + \chi_{mn}^2}{k_0 \chi_{mn}} \overline{Q}_{mn} P_{mn} \approx \frac{4g_x}{\pi d_x} - i g_x^2 \frac{4k_0}{a\pi^2} \overline{\Omega}, \tag{1.19}$$

where

$$\Omega \equiv \ln\left(\frac{2g_x \pi}{d_x} \right) - \frac{3}{2},$$

$$\overline{\Omega} \equiv \left[\ln\left(\frac{2\pi(\mathrm{w} + g_x)}{d_x} \right) + \frac{2\mathrm{w}}{g_x} \ln\left(\frac{2\pi(\mathrm{w} + g)}{d_x} \right) + \frac{\mathrm{w}^2}{g_x^2} \ln\left(\frac{\mathrm{w} + g_x}{\mathrm{w}} \right) - \frac{3\mathrm{w}}{g_x} - \frac{3}{2} \right].$$

The followings can be obtained explicitly from Eq. (1.18):

$$\begin{aligned}
A_1 + B_1 &= \frac{1}{\eta_1} \left[-\overline{W} \cos\left(\frac{k_0 h}{2} \right) + \frac{4}{\pi} \left(V \cos\left(\frac{k_0 h}{2} \right) - i \sin\left(\frac{k_0 h}{2} \right) \right) \right], \\
A_1 - B_1 &= \frac{1}{\eta_2} \left[i\overline{W} \sin\left(\frac{k_0 h}{2} \right) + \frac{4}{\pi} \left(-iV \sin\left(\frac{k_0 h}{2} \right) + \cos\left(\frac{k_0 h}{2} \right) \right) \right], \\
A_2 + B_2 &= \frac{1}{\eta_1} \left[\left(W \cos\left(\frac{k_1 h}{2} \right) - i \sin\left(\frac{k_1 h}{2} \right) \frac{k_1}{k_0} \right) - \frac{4}{\pi} \overline{V} \cos\left(\frac{k_1 h}{2} \right) \right], \\
A_2 - B_2 &= \frac{1}{\eta_2} \left[\left(-iW \sin\left(\frac{k_1 h}{2} \right) + \cos\left(\frac{k_1 h}{2} \right) \frac{k_1}{k_0} \right) + i \frac{4}{\pi} \overline{V} \sin\left(\frac{k_1 h}{2} \right) \right],
\end{aligned} \tag{1.20}$$

with

$$\eta_1 \equiv \left(W \cos\left(\frac{k_1 h}{2} \right) - i \sin\left(\frac{k_1 h}{2} \right) \frac{k_1}{k_0} \right) \left(V \cos\left(\frac{k_0 h}{2} \right) - i \sin\left(\frac{k_0 h}{2} \right) \right) - \overline{V}\overline{W} \cos\left(\frac{k_0 h}{2} \right) \cos\left(\frac{k_1 h}{2} \right),$$

$$\eta_2 \equiv \left(iW \sin\left(\frac{k_1 h}{2} \right) - \cos\left(\frac{k_1 h}{2} \right) \frac{k_1}{k_0} \right) \left(iV \sin\left(\frac{k_0 h}{2} \right) - \cos\left(\frac{k_0 h}{2} \right) \right) - \overline{W}\overline{V} \sin\left(\frac{k_0 h}{2} \right) \sin\left(\frac{k_1 h}{2} \right).$$

2. Resonance condition

The deep sub-wavelength thickness and lattice spacing of the metasurface allows to approximate Eq. (1.12) and (1.20). By expanding up to linear terms of k_0h, k_1h, and gh, we have an approximated form of Eq. (1.12) as

$$\begin{aligned} T_{y,00} &\approx \frac{2ab}{d_x d_y \pi}\left[A_1 + B_1 + \left(A_1 - B_1\right)\frac{ik_1 h}{2}\right] + \frac{g_x}{d_x}\left[A_2 + B_2 + \left(A_2 - B_2\right)\frac{ik_0 h}{2}\right], \\ R_{y,00} &\approx 1 - \frac{2ab}{d_x d_y \pi}\left[A_1 + B_1 - \left(A_1 - B_1\right)\frac{ik_1 h}{2}\right] - \frac{g_x}{d_x}\left[A_2 + B_2 - \left(A_2 - B_2\right)\frac{ik_0 h}{2}\right]. \end{aligned} \tag{2.1}$$

Equation (1.20) can be also approximately written as

$$\begin{aligned} &A_1 + B_1 \approx \frac{1}{\pi\eta_1}\left[-\pi W + 4V - 2ik_0 h\right], \quad A_1 - B_1 \approx \frac{4k_0}{\pi k_1}, \\ &A_2 + B_2 \approx \frac{1}{\pi\eta_1}\left[\pi W - i\pi\frac{k_1^2 h}{2k_0} - 4V\right], \quad A_2 - B_2 \approx 1, \\ &\eta_1 \approx WV - iW\frac{k_0 h}{2} - iV\frac{k_1^2 h}{2k_0} - VW. \end{aligned} \tag{2.2}$$

Then, by putting Eq. (2.2) into Eq. (2.1), we arrive at simplified zero-th order transmission coefficient that are necessary to define the resonance condition:

$$\begin{aligned} &T_{y,00} \approx F + i\sigma \\ &F \equiv \frac{1}{\pi\eta_1}\left[\frac{2ab}{d_x d_y \pi}\left(-\pi W + 4V - 2ik_0 h\right) + \frac{g_x}{d_x}\left(\pi W - i\pi\frac{k_1^2 h}{2k_0} - 4V\right)\right], \\ &\sigma \equiv k_0 h\left(\frac{4ab}{d_x d_y \pi^2} + \frac{g_x}{2d_x}\right). \end{aligned} \tag{2.3}$$

Note that σ is real-valued and very small when $h, g_x << a, b$. Now, we find the resonance condition by examining the requirement for the vanished transmittance. From Eq. (2.3), the vanished transmittance can be written as

$$|T_{y,00}|^2 \approx |F|^2 + 2\,\mathrm{Re}(F)\sigma \approx \mathrm{Re}(F) + 2\,\mathrm{Im}(F)\sigma = 0. \tag{2.4}$$

In Eq. (2.4), we neglected the contribution from σ^2 and used an approximation $|F|^2 \approx \mathrm{Re}(F)$ that can be found from Eq. (1.12) and the lossless condition $|T|^2 + |R|^2 = 1$. Also, by using the fact that $\pi\,\mathrm{Re}(W) = 4\,\mathrm{Re}(\overline{V})$ and $\pi\,\mathrm{Re}(\overline{W}) = 4\,\mathrm{Re}(V)$, we can rewrite Eq. (2.4) as

$$\mathrm{Re}(F) + 2\,\mathrm{Im}(F)\sigma = \mathrm{Im}(\eta_1) + 2\sigma\,\mathrm{Re}(\eta_1) \tag{2.5}$$

Therefore, the resonance condition can be approximately found by evaluating η_1 and letting $\mathrm{Im}(\eta_1)+2\sigma\mathrm{Re}(\eta_1)=0$. From Eq. (1.19) and (2.2), one can find that the real and imaginary parts of η_1 can be written as

$$\begin{aligned}
\mathrm{Re}(\eta) &\approx -\frac{4ad_y^2 g_x}{\pi^2 b^3 d_x}\Omega + \frac{2ahd_y^2}{\pi b^3 d_x}, \\
\mathrm{Im}(\eta) &\approx \frac{8ab}{\pi^2 d_x d_y}\left[\frac{g_x k_0}{\pi}\Omega + \frac{\pi g_x d_y^3}{2d_x b^4}\frac{1}{k_0} - \frac{k_0 h}{2}\right].
\end{aligned} \tag{2.6}$$

Substituting Eq. (2.6) into (2.5) gives the resonance condition as

$$\frac{g_x k_0}{\pi}\left(\ln\left(\frac{2\pi g_x}{d_x}\right) - \frac{3}{2}\right) + \frac{\pi g_x d_y^3}{2d_x b^4}\frac{1}{k_0} - \frac{k_0 h}{2} + k_0 h\left(1 + \frac{g_x \pi^2 d_y}{8ab}\right)\left(-\frac{4ad_y^2 g_x}{\pi^2 b^3 d_x}\Omega + \frac{2ahd_y^2}{\pi b^3 d_x}\right) = 0. \tag{2.7}$$

Note that $\Omega \equiv \ln\left(2\pi g_x / d_x\right) - 3/2$. For deep sub-wavelength thickness and lattice spacing, $h, g_x << a, b < \lambda$, the last term of the left-hand-side of Eq. (2.7) can be suppressed. Then, we finally arrive at simplified resonance condition:

$$\frac{h\pi}{g_x} - 2\ln\left(\frac{2\pi g_x}{d_x}\right) - \frac{\lambda^2 d_y^3}{4 d_x b^4} + 3 = 0. \tag{2.8}$$

Or equivalently, the resonance wavelength can be found as

$$\lambda_{res} = \frac{2b^2}{d_y}\sqrt{\frac{d_x}{d_y}}\sqrt{\frac{h\pi}{g_x} - 2\ln\left(\frac{2g_x\pi}{d_x}\right) + 3}. \tag{2.9}$$

3. Macroscopic channel competition

The lattice-spacing-dependent resonance condition we have discussed so far is based on the behavior of transmission amplitude of incident light. For the sake of deeper physical interpretation of the resonance, it is worth focusing on some macroscopic near-field features. Let's revisit the transmission coefficient in Eq. (1.12):

$$T_{y,00} = \frac{2ab}{d_x d_y \pi}\left[A_1 e^{ik_1 h/2} + B_1 e^{-ik_1 h/2}\right] + \frac{g_x}{d_x}\left[A_2 e^{ik_0 h/2} + B_2 e^{-ik_0 h/2}\right]. \tag{3.1}$$

One can readily find that Eq. (3.1) can rewrite as

$$T_{y,00} = \left(\int_{c^{(1)}} dxdy + \int_{c^{(2)}} dxdy\right)\frac{E_{xII}(x,y)}{d_x d_y}. \tag{3.2}$$

Explicit evaluation of the integral over the channel $c^{(1)}$ by using Eqs. (2.1)-(2.3) gives rise to

$$\overline{E_x^{(1)}} \equiv \int_{c^{(1)}} \frac{E_{xII}}{d_x d_y} dxdy \,|_{z=0} \approx \frac{2ab\omega^2}{\pi d_x d_y} \times \frac{\left(\omega^2 - \omega_{res}^2\right) - i\alpha}{\left(\omega^2 - \omega_{res}^2\right)^2 + \alpha^2}, \tag{3.3}$$

where $\alpha \equiv \pi d_y^3 \omega^2 / \left(2b^4 k_0\right) > 0$, $\omega \equiv 2\pi c_0 / \lambda$, $\omega_{res} \equiv 2\pi c_0 / \lambda_{res}$, and c_0 is the speed of light in vacuum. In Eq. (3.3), we can find that the sign of $\mathrm{Re}\left(\overline{E_x^{(1)}}\right)$ changes at the resonance, while that of $\mathrm{Im}\left(\overline{E_x^{(1)}}\right)$ does not change. Explicit evaluation of the integral over the second channel $c^{(2)}$ exhibits the same trend except for that overall sign is opposite to the $c^{(1)}$ case. Combining these facts, we can restate the resonance condition in terms of lattice-averaged electric field components by

$$\mathrm{Re}\left(\overline{E_x^{(1)}}\right) = \mathrm{Re}\left(\overline{E_x^{(2)}}\right) = 0, \quad \mathrm{Im}\left(\overline{E_x^{(1)}}\right) + \mathrm{Im}\left(\overline{E_x^{(2)}}\right) = 0. \tag{3.4}$$

All those trends are shown in Fig. S3(a) which plots lattice-averaged field components as functions of lattice spacing. On the other hand, one can find that the magnetic field components in each channel can be approximately written as

$$H_{yII}^{(1)} \approx \sqrt{\frac{\varepsilon_0}{\mu_0}} \frac{4}{\pi} \sin\left(\frac{\pi y}{b}\right), \quad H_{yII}^{(2)} \approx \sqrt{\frac{\varepsilon_0}{\mu_0}}, \tag{3.5}$$

with negligible imaginary parts as shown in Fig. S3(b). Therefore, the total energy flux through the metasurface system, equivalent to the z-component of the time-averaged Poynting vector $< \vec{S} > \equiv \mathrm{Re}(\vec{E} \times \overrightarrow{H}^* / 2)$, can be simplified as $<S_z> \approx \mathrm{Re}(E_x) H_y / 2$. This gives rise to an intuitive criterion for the resonance condition through

$$\begin{aligned}
&\left\langle S_z^{(1)} \right\rangle > 0, \quad \left\langle S_z^{(2)} \right\rangle < 0, \quad \text{for } g < g_t, \\
&\left\langle S_z^{(1)} \right\rangle < 0, \quad \left\langle S_z^{(2)} \right\rangle > 0, \quad \text{for } g > g_t \\
&\left\langle S_z^{(1)} \right\rangle = \left\langle S_z^{(2)} \right\rangle = 0, \quad \text{for } g = g_t.
\end{aligned} \tag{3.6}$$

The incident light transmits through the channel $c^{(1)}$ when $g<g_t$, and otherwise the incident light chooses channel $c^{(2)}$ to pass through the metasurface. Therefore, the resonance is a result of the competition between those two channels to admit incident light. As shown in Fig. S4, our interpretation perfectly agrees with FDTD results.

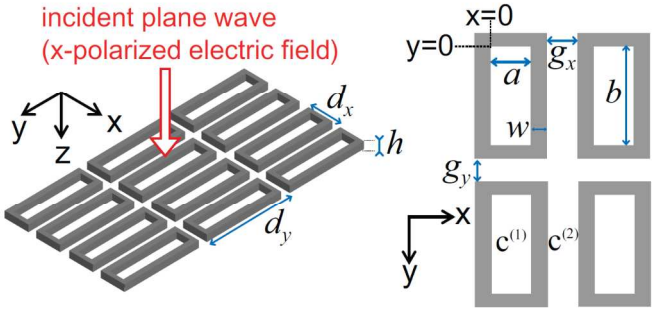

Fig. S1. Schematics of our metasurface. $c^{(1)}$ and $c^{(2)}$ denote the two dominant light channels in the metasurface.

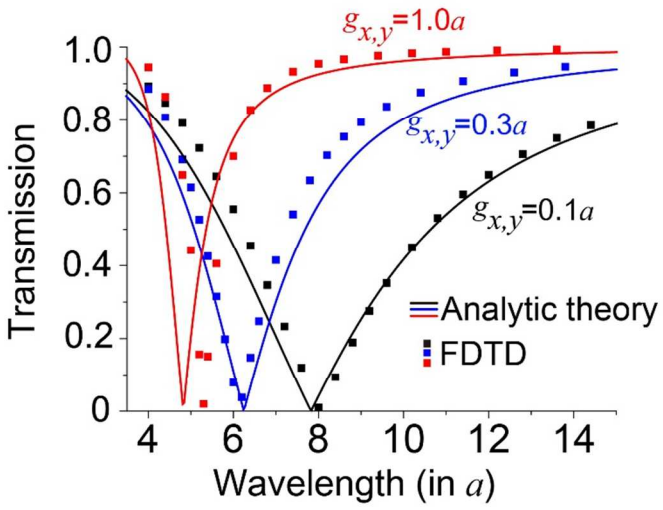

Fig. S2. Lattice-spacing-dependent transmission spectra in loosely-coupled metasurfaces. We set b=2a, w=0.04a, and h=0.1a.

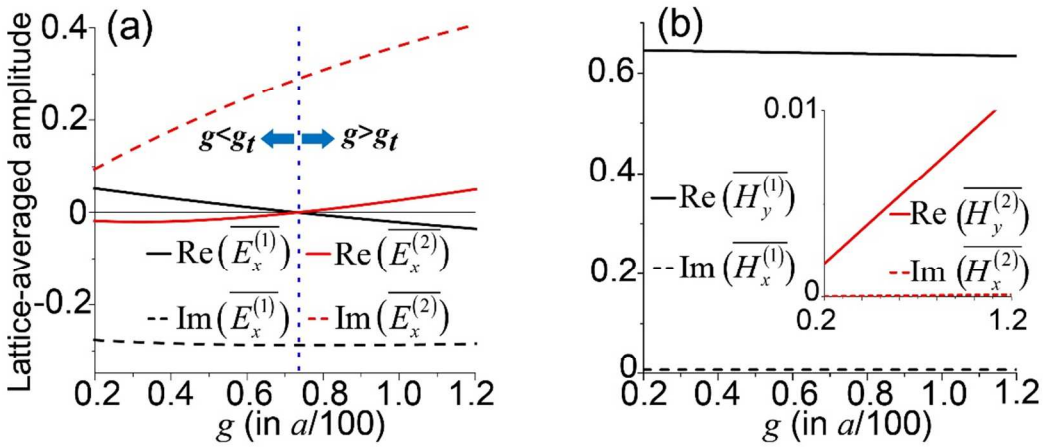

Fig. S3. Lattice-averaged (a) E_x and (b) H_y at z=0 for two light channels. Blue dotted line in (a) denotes the critical lattice spacing g_t, calculate by Eq. (2.8). We set b=a, w=0.05a, and h=0.05a, and λ=10a.

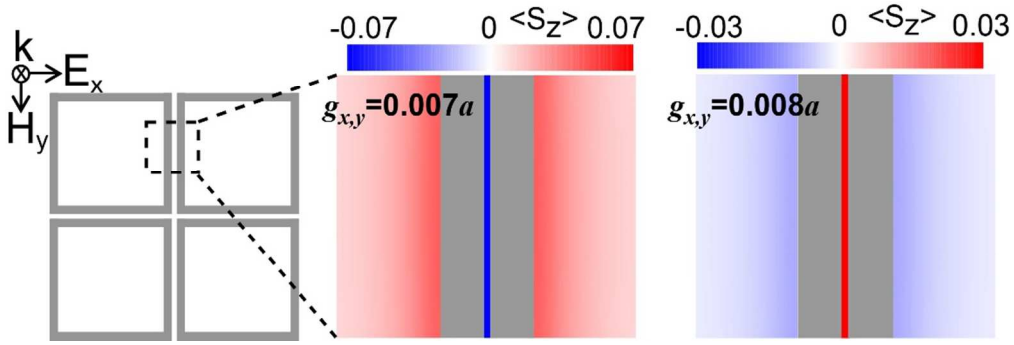

Fig. S4. FDTD-calculated maps of the time-averaged Poynting vectors through metasurfaces with two different lattice spacing sizes. We considered the same geometric parameters used in Fig. S3.

References

[1] J. H. Kang, J. H. Choe, D. S. Kim, and Q. H. Park, Optics Exp. **17**, 15652 (2009).

[2] F. J. Garcia-Vidal, L. Martín-Moreno, T. W. Ebbesen, and L. Kuipers, Rev. Mod. Phys. **82**, 729 (2010).